LA-UR- 00-3903

Approved for public release;
distribution is unlimited.

Title: IDENTIFICATION OF NONLINEARITIES IN AN 8-DOF SYSTEM THROUGH SPECTRAL FEEDBACK

Author(s): Benjamin Arcand, LANL
Michigan Technological University
Mechanical Engineering

Jeannette R. Wait, LANL
USC, Civil Engineering Department

Submitted to: International Modal Analysis Conference
Orlando, FL
February 5 - 8, 2001

Los Alamos
NATIONAL LABORATORY

Form 836 (8/00)

DISCLAIMER

IDENTIFICATION OF NONLINEARITIES IN AN 8-DOF SYSTEM THROUGH SPECTRAL FEEDBACK

Jeannette R. Wait[1], Benjamin Y. Arcand[2], Jonathan E. Webster[3], Norman F. Hunter [4]

[1]Department of Civil Engineering, MS 2531, University of Southern California, Los Angeles, CA, 90089
[2]Department of Mechanical Engineering, 1400 Townsend Dr., Michigan Tech. University, Houghton, MI, 49931
[3]Department of Mathematics & Computer Engineering, Rose-Hulman Inst. of Technology, Terre Haute, IN, 47803
[4]Measurement Technology Group, MS C931, Los Alamos National Laboratory, Los Alamos, NM, 87545

ABSTRACT

The accurate detection and characterization of nonlinearities associated with damage in structural systems is an area of vibration analysis that is being widely researched. In this paper, nonlinear behavior is considered a potential indicator of damage. Most conventional damage detection methods, such as those based on resonant frequencies and mode shapes, do not accurately identify the location and extent of nonlinearities present in a given structural system. As an extension of previous work at LANL, an effort is made to validate a damage detection method proposed by Adams [1]. This method states that the frequency response function (FRF) matrix obtained from a low-level vibration test approximates the underlying linear FRF matrix of the system. The nonlinear systems' responses to high level excitation are combined with the linear FRF in a classic feedback loop to obtain the contributions of nonlinear internal forces. The temporal and spatial characteristics of the nonlinearities present in a structural system are identified. An 8-DOF system is used as a test case to validate the aforementioned method. Results of the tests and important issues concerning the method are presented.

NOMENCLATURE

The following are adapted from [1]:

$\{X(\omega)\}_{No\,x\,1}$	Linear Fourier spectrum of the output vector of a nonlinear system
N_o	Number of outputs
$\{F(\omega)\}_{No\,x\,1}$	Fourier spectrum of the input vector
$[I]$	The identity matrix
$[H_L(\omega)]_{No\,x\,No}$	Frequency response function matrix of a linear system
$X_{ni}(\omega)$	Scalar nonlinear function of the outputs for nonlinear element i
$X_{NL}(\omega)$	Fourier spectrum of the outputs from the nonlinear system
$[B_L(\omega)]_{No\,x\,No}$	Impedance matrix of a linear or linearized system
$[_xB_{ni}(\omega)]_{No\,x\,No}$	Frequency response (projection) matrix between the outputs and $X_{ni}(\omega)$ associated with the nonlinear element i
$[_fB_{ni}(\omega)]_{No\,x\,No}$	Frequency response (projection) matrix between the external inputs and $X_{ni}(\omega)$ associated with the nonlinear element i
$\{B_{ni}(\omega)\}_{No\,x\,No}$	Vector of impedance with nonlinear coefficient and nonlinear spectral function factored out to yield entries of 1 and −1 only; associated with nonlinear element i
$\mu_i(\omega)$	Scalar nonlinear parameter for nonlinear element i
$[B_M(\omega)]_{No\,x\,No}$	$\mu_i(\omega)\{B_{ni}(\omega)\}_{No\,x\,No}$
DOF	Degree-of-freedom
FRF	Frequency response function
$[_xH_M(\omega)]_{No\,x\,No}$	Nonlinear modulation matrix on the outputs
$[_xH(\omega)]_{No\,x\,No}$	Frequency response function matrix using the projection onto the outputs

1. INTRODUCTION

The ability to identify and characterize damage (nonlinear elements) in a structural system is of great importance in the aerospace, civil engineering, and mechanical engineering industries. Over the past two decades, this area of vibration-based research has concentrated on damage detection methods for various structures including, but not limited to cracks in beams, plates, scaled models of multi-story buildings, and frames [2]. The goal is the detection, identification and repair of damage present in a structural system before failure occurs.

Most current damage detection methods define damage to be changes in the dynamic response of the system that alter the mass, stiffness, or energy dissipation of the structure. The majority of the methods to date are based on changes in resonant frequencies and mode shapes. A few methods also use neural networks, changes in flexibility, and statistical models, but these are not as well researched as those based on shifts in frequency and changes in mode shapes.

There are several problems associated with the use of frequency-based damage detection methods. In order to use most frequency-based methods, the dynamic characteristics of the structure must be known prior to damage. In other words, data must be available for the initial, undamaged state of the system. This is a problem for older structures that were not instrumented during construction. In addition to requiring data from both the undamaged and damaged system, a large number of frequency methods also assume that the damaged area of a structure is known *a priori* [2]. Therefore, unless these frequency-based methods are being implemented to identify damage that is already known, then a majority of the methods available become useless when the **location** of damage is one of the unknowns.

If both the location of the damage and the data from the undamaged system are available, there are still problems with frequency-based methods. The difficulty then becomes being able to excite the structure in a frequency range that will excite the damage. Typically, damage is a local phenomenon which implies that the lower-frequency global response (which is most often measured) is less influenced by any damage present in a system. In order to detect damage, structures need to be excited in a much higher frequency range. In a laboratory setting, this might not be a problem, but for large-scale tests it is difficult to excite a structure in the necessary range due to the amount of energy required to produce a good response [2].

Data compression is another drawback of not only frequency and modal-based testing, but also any vibration-based test that implements post-processing of data acquired. Data are commonly windowed and averaged to avoid leakage and obtain a clearer visualization of the dynamic response of the system in the frequency domain. Although this may provide cleaner modal data, a lot of information about the structure is potentially lost through the data reduction process. But without the use of data reduction, the data will most likely be too complex to accurately analyze. Therefore, most researchers take opt to use data compression methods and rely mostly on the modal properties obtained to identify damage present in structural systems [2,3]. Data compression is essential, but it is critical to implement compression algorithms that retain damage sensitive features of the data.

Finally, a problem that is prevalent in all types of vibration-based damage detection methods is the fact that very few have been implemented on full-scale *in-situ* structures. Most available methods have been implemented in a laboratory setting on scaled models such as beams and plates. The major reason this problem exists is due to the lack of full-scale structures that are available for destructive testing [4].

The damage detection method implemented in this paper (and presented in [1]) is based upon frequency data, but does not contain the majority of the aforementioned "problems" with frequency-based vibration tests. Specifically, Adams' method does not depend on; changes in resonant frequencies or mode shape, the undamaged state of the system, or prior knowledge of the damage location(s).

In the following sections, Adams' method will be presented and then applied to an 8-dof mass-spring system. Examples of results and issues concerning the implementation of the method in question will also be discussed.

2. ADAMS' THEORY

2.1 Overview of Adam's Method

Adams presents a new method for detection, classification, and location of nonlinear elements in a given system [5]. His focus is on a derivation of the frequency response function [1], and on a superposition principle for nonlinear systems [5].

The input data, output data, and the number of degrees-of-freedom make up an experimental system description. The key to Adams' method is that it views the nonlinearity as an internal force, which acts together with external forces on the underlying linear system [1]. Known effects of the linear FRF are removed from the nonlinear behavior, isolating the nonlinear force.

In real systems one typically has fewer inputs than outputs. Normally, the lumped parameter model of the system would look like

$$\{X(\omega)\}_{Nox1} = [H_L(\omega)]_{NoxNi}\{F(\omega)\}_{Nix1} \quad (1)$$

where *No* is the number of outputs and *Ni* is the number of inputs. To allow nonlinear forces at each response locations, the lumped parameter model equations are written as

$$\{X(\omega)\}_{Nox1} = [H_L(\omega)]_{NoxNo}\{F(\omega)\}_{Nox1} \quad (2)$$

By keeping track of the outputs, Adams' method treats the nonlinearities as hidden inputs. These inputs are unmeasured, internal, feedback forces that are nonlinear functions of the output [1]. Use of multiple inputs and multiple outputs (MIMO) also aids in tracking these nonlinearities.

2.2 Using the Feedback Loop and the MIMO system

The model in equations (1), (2) is inappropriate for nonlinear systems. The linear and nonlinear dynamics combine creating an FRF matrix of the nonlinear system that is different from the FRF matrix of the linear system [1]. This prompted Adams to view the nonlinearity as a lumped

element. In the frequency domain, the total system model is:

$$\{B_L(\omega)\}_{NoxNo}\{X(\omega)\}_{Nox1} + \mu_1(\omega)\{B_{n1}\}_{Nox1} X_{NL}(\omega) = \{F(\omega)\}_{Nox1} \quad (3)$$

In this impedance model, $[B_L(\omega)]$ is the linear impedance. The nonlinear portions are found in the vector $\mu_1(\omega)\{B_{n1}\}X_{NL}(\omega)$. $X_n(\omega)$ is the scalar that determines the class of the nonlinearity. $\{B_{n1}\}$ has three possible values, 0, -1, 1, which determine the location of the nonlinearity. The final term, $\mu_1(\omega)$, quantifies the strength of the feedback force. The vector $\mu_1(\omega)\{B_{n1}\}X_{NL}(\omega)$ describes one nonlinearity. A generalization of this sums many such nonlinear vectors.

The FRF matrices of the linear system couple the nonlinear and linear mechanics. Use of the impedance relationship

$$B_L(\omega) = \frac{1}{H_L(\omega)} \quad (3a)$$

avoids much of this coupling. The internal feedback forces are functions of the outputs [1]. In equation (4) below, N_n nonlinearities are allowed.

$$\{B_L(\omega)\}_{NoxNo}\{X(\omega)\}_{Nox1} + \sum_{i=1}^{N_n}\mu_i(\omega)\{B_{ni}\}_{Nox1} X_{ni}(\omega) = \{F(\omega)\}_{Nox1} \quad (4)$$

Reviewing (4):

$$\{B_L(\omega)\}_{NoxNo}\{X(\omega)\}_{Nox1} = \{F(\omega)\}_{Nox1} - \sum_{i=1}^{N_n}\mu_i(\omega)\{B_{ni}\}_{Nox1} X_{ni}(\omega). \quad (5)$$

Adams notes that if you ignore the nonlinear terms in (5), the equation becomes linear [1]. In a real system assumed to be linear, the nonlinear terms just contribute noise or other errors that are ignored.

At every frequency $\{B_{ni}\}_{Nox1}X_{ni}(\omega)$ is a linear combination of the response vector components of $\{X(\omega)\}$. This gives the MIMO, spectral, total least-squares set of equations:

$$\{B_{ni}(\omega)\}_{Nox1} X_{ni}(\omega) = [{}_x B_{ni}(\omega)]_{NoxNo}\{X(\omega)\}_{Nox1} \quad (6)$$

Equation (6) describes the nonlinear behavior as a function of measured responses. As Adams notes, the nonlinear behavior can also be described as a function of the measured external forces.

$$\{B_{ni}(\omega)\}_{Nox1} X_{ni}(\omega) = [{}_f B_{ni}(\omega)]_{NoxNo}\{F(\omega)\}_{Nox1} \quad (7)$$

Equation (7) eliminates the unmeasured internal forces in favor of the measured external forces [1].

By combining equations (4) and (6)

$$\{B_L(\omega)\}_{NoxNo}\{X(\omega)\}_{Nox1} + [B_n(\omega)]_{NoxNo}\{X(\omega)\}_{Nox1} = \{F(\omega)\}_{Nox1}. \quad (8)$$

The entire summation is replaced with a single impedance matrix, $[B_n(\omega)]$. In figure (1) it is easy to see the feedback nature of this equation.

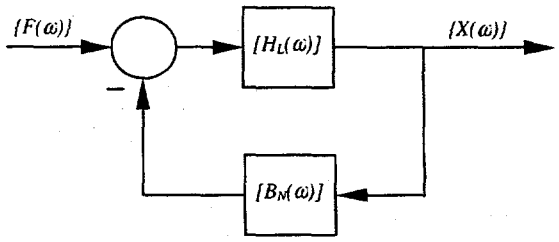

Figure 1: Closed loop representation of equation (8)

2.3 Locating the Damage

If the system is purely linear, the loop is unnecessary. When considering a nonlinear system with damage present, the closed loop model with feedback of the internal forces is applicable.

In [1], Adams defines three equations

$$\{X(\omega)\}_{N_o x1} = [[I]_{N_o x N_o} + [H_L(\omega)]_{N_o x N_o}[B_n(\omega)]]^{-1}\{F(\omega)\}_{N_o x1} \quad (9)$$

$$\{X(\omega)\} = [{}_x H_M(\omega)][H_L(\omega)]_{NoxNo}\{F(\omega)\} \quad (10)$$

$$\{X(\omega)\} = [{}_x H(\omega)]\{F(\omega)\} \quad (11)$$

Using these equations, it is possible to calculate, locate, and describe a nonlinearity present in a system.

The matrix $[{}_xH(\omega)]$ is the modulation matrix that determines the strength and location of the nonlinearity. As the system becomes more linear this matrix approaches the identity matrix [5]. This is used to determine the strength of the nonlinearity.

The rows of the modulation matrix determine the location of the nonlinearity. Each row corresponds to one of the degrees-of-freedom, so if two rows have significant values present in them, then the nonlinearity is located between those degrees-of-freedom [5].

3. APPLICATION TO AN 8-DOF SYSTEM

3.1 Description of 8-DOF System

In an attempt to validate Adams' method, an experiment was performed on an 8-dof system that consisted of eight masses and seven springs connected in series. Uniaxial accelerometers were attached to each of the eight masses. A force transducer located at the base of the configuration recorded the force input to the system (See Figure 2). In order to mount the mass-spring system vertically, it was threaded through a stainless steel bar which was attached to a steel frame (See Figure 2). The stainless steel bar introduced coulomb friction into the system. The mass-spring system would tend to "stick and then slip" along the

bar. To minimize this affect, the stainless steel bar was lubricated with Tri-Flo, a common commercial lubricant, before the masses and springs were installed for each test.

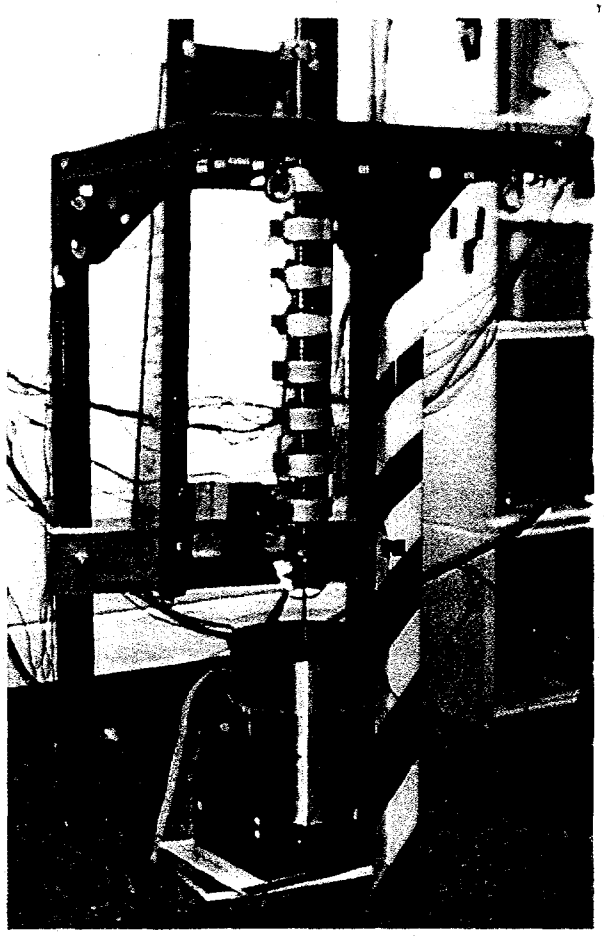

Figure 2: 8-DOF Experiment Setup

A more detailed diagram of the mass-spring system is shown in Figure 3 and the nominal values of the eight masses and seven springs are listed in Table 1.

Nominal Values of Masses			Spring Constants	
Unit	M1	M2-M8	Unit	K1-K7
kg	0.5593	0.4194	Kn/m	56.7

Table 1: Values of Masses and Springs

To introduce a nonlinearity into the 8-dof system, two bumpers consisting of tiny steel bars were attached to one of the masses. Rather than having a metal-metal contact when the bumpers hit, "bumper contacts" were made out of a dense polymer that fit inside the head of a hex screw. This provided a better contact surface (See Figure 4).

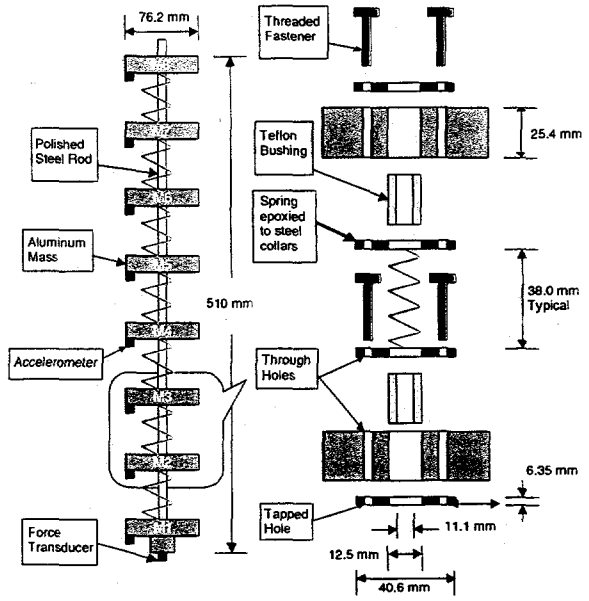

Figure 3: Detailed diagram of mass-spring system

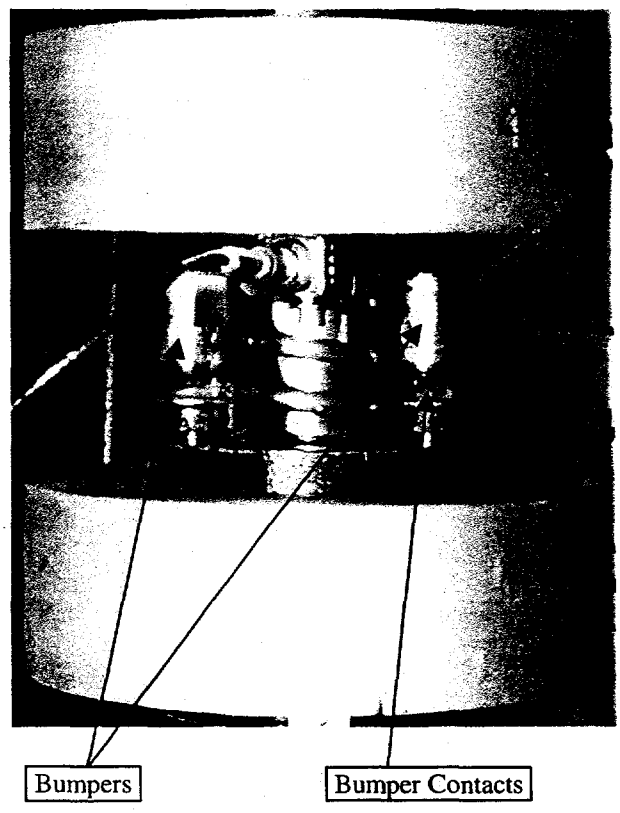

Figure 4: View of Bumpers and Bumper Contacts

3.2 Equipment Used

The following equipment were used during the tests of the 8-dof system. Tables 2 and 3 contain the specifications of the sensors used.

1. 40 channel HP3566A/67A data acquisition system
   a. 35653A 50 kHz input source

b. 35651C signal processor
2. TECHRON 5530 power amplifier
3. Vibration Test Systems, VG 100-6 electromagnetic shaker
4. Endevco 2251-A ISOTRON® PE Accelerometers
5. PCB 208A04 piezoelectric force transducer
6. Matlab v. 5.3 R11.1
7. IBM ThinkPad Pentium Laptop

Accelerometer Position	Serial Number	Channel Number	Sensitivity (mv/g)
M1	DF39	2	9.873
M2	DE60	3	10.06
M3	DG78	4	9.561
M4	DF53	5	9.696
M5	DF10	6	9.851
M6	DG77	7	9.605
M7	DE94	8	10.04
M8	DF43	9	9.439

Table 2: Specifications for Endevco 2251A-10 ISOTRON® PE Accelerometers

Force Transducer Serial Number	Channel Number	Sensitivity (lbf/V)
2041	1	1.000

Table 3: Specification for PCB 208A04 Piezoelectric Force Transducer

3.3 Description of Experiment

For all tests, a 10V random excitation was generated by the HP3566A, amplified by the TECHRON power amplifier, and input to the 8-dof system at the base of the structure (below mass 1). Two separate tests were run to obtain both the linear and nonlinear dynamic responses of the system. The first test was run without any bumpers installed to capture the linear. Then the bumpers were installed between two particular masses to obtain nonlinear data. Several separate tests were taken with the bumpers in different locations to provide a larger data set for analysis purposes. For both the linear and nonlinear setups, the outputs of all accelerometers and the force transducer were recorded by the HP3566A and saved for post-processing.

3.4 Data Acquisition and Processing

Time domain data were acquired for 32-seconds, sampled at 1024 samples per second. Data were then saved to disk and converted to universal file format for post-processing. Each time file consisted of eight acceleration time histories and one input force time history with 32768 samples per channel.

The Signal Analysis Toolbox within Matlab was used to post-process [6] the time data. The data were processed using traditional FFT analysis techniques using spectral windowing and overlap processing. The FRFs and coherence functions were calculated with the tfe and cohere functions respectively with an fft size of 1024, sample rate of 1024, a hanning window, and a 50% overlap.

Generally speaking, the use of the hanning window helps prevent leakage of data. Specifically, the hanning window attenuates the input signal by bringing both ends of each block of data to zero. This removed end-of-block discontinuities in the signal. In Fourier series analysis, any discontinuities in the time domain signal are represented by a large number of low and high frequencies. As a result, the output generated contains many high frequency components. By using the hanning window, and thus removing the high frequency components in the input signal, the high frequency components in the output data were attenuated. The removal of the extraneous side band frequencies that occur as a result of the discontinuities produced data that were more representative of the actual output data.

3.5 Implementing Adams' Method

Equations (9) and (11) are the primary equations used in solving for the known nonlinearities in the 8-dof system. Equation (12) is formed by left multiplying the term that is inversed in equation (9):

$$\{X(\omega)\}_{N_o x1} + [H_L(\omega)]_{N_o x N_o}[B_{ni}(\omega)]\{X(\omega)\}_{N_o x1} = [H_L(\omega)]_{N_o x N_o}\{F(\omega)\}_{N_o x1}. \quad (12)$$

Subtracting $\{X(\omega)\}_{Nox1}$ from each side of the equation forms

$$[H_L(\omega)]_{NoxNo}[B_n(\omega)]_{NoxNo}\{X(\omega)\}_{Nox1} = \{\Delta\}_{Nox1}. \quad (13)$$

Here, $\{\Delta\}$, is the difference between the computed Fourier spectrum of the outputs and the measured Fourier spectrum of the outputs. Computed outputs are based on the underlying linear FRF of the nonlinear system. The difference between the measured and computed responses represents the contribution of nonlinear internal forces.

Since $\{X(\omega)\}_{Nox1}$ and $\{H_L(\omega)\}_{NoxNo}\{F(\omega)\}_{Nox1}$ are known, $\{\Delta\}$ can be obtained. By taking successive blocks of data and using a linear regression technique, the product $[H_L(\omega)]_{NoxNo}[B_n(\omega)]_{NoxNo}$ is estimated.

Alternatively, equation (11) can be solved for the estimate of the nonlinear frequency response function matrix projected onto the outputs, $[_xH(\omega)]$. This produces the same results as those given by solving for $[H_L(\omega)]_{NoxNo}[B_n(\omega)]_{NoxNo}$ in equation (12).

The 8-dof system was excited by a single input at the base of the stainless steel bar beneath mass 1 (See Figure 2). Equations (10) and (12) require that the FRF matrix due to the underlying linear system, $[H_L(\omega)]_{NoxNo}$, be $N_o x N_o$. This requires an input at each of the degrees of freedom. With a single input, the FRF matrix of the underlying linear system is $N_o x 1$. In [5], Adams' method is applied to a system with a single input and multiple outputs. There might be slight errors in the results due to numerical instability of the inverse in equation (9), but the nonlinearities present can still be identified.

3.6 Results of Experiment

As described in Section 3.5, both the product $[H_L(\omega)]_{NoxNo}[B_n(\omega)]_{NoxNo}$, and the matrix $[_xH(\omega)]$, were calculated from the 8-dof experimental data. Sample plots of these two matrices for damage between masses 3 and 4 are

shown below (See Figures 5 and 6). Each plot shows the two matrices as functions of position and frequency.

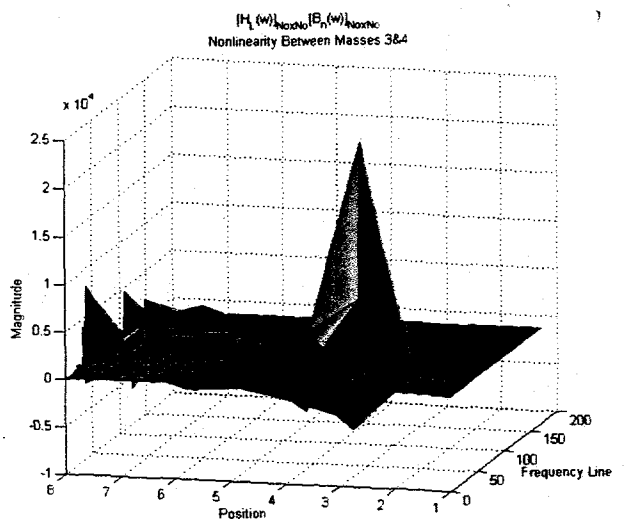

Figure 5: $[H_L(\omega)]_{NoxNo}[B_n(\omega)]_{NoxNo}$ Matrix Showing Nonlinearity Present Between Masses 3 & 4

The largest magnitude occurs between positions 3 and 4 in both figures. The peak magnitudes in these plots indicate how much $[H_L(\omega)]_{NoxNo}[B_n(\omega)]_{NoxNo}$ and $[_xH(\omega)]$, respectively, differ from the identity matrix. The peak magnitude between positions 3 and 4 corresponds to a nonlinearity present between masses 3 and 4.

Some of the results detect the known nonlinearity present for a given location, but not all scenarios tested were accurately identified by either method discussed in the previous section. For example, Figure 5, shows the accurate identification (using equation (12)) of a nonlinearity present between masses 3 and 4. The same method, applied when the induced nonlinearity was between masses 2 and 3 does not show a peak between locations 2 and 3 (See Figure 7). The same is true when solving for $[_xH(\omega)]$. Figure 8 shows the plot of $[_xH(\omega)]$ for a nonlinearity located between masses 4 and 5. This clearly indicates that the results from the 8-dof experiments are inconclusive.

Due to the results discussed above and shown in the previous figures, it is concluded that the methods presented in [1] and [5] do not consistently identify nonlinearities in the 8-dof system tested.

There are several reasons why the application of Adams' method produced inconclusive results for the 8-dof system discussed in this paper.

1. The 8-dof system, without the bumpers installed, was not linear. The stainless steel bar that kept the mass-spring system vertical, introduced a nonlinearity (in the form of friction) into the system. The underlying linear FRF that was measured, $[H_L(\omega)]$, was therefore not an accurate measurement. This was actually a measurement of a nonlinear system. The nonlinearity had an unpredictable effect on calculations of equations (9) and (11). Theses calculations were therefore based on the FRF of a nonlinear system.

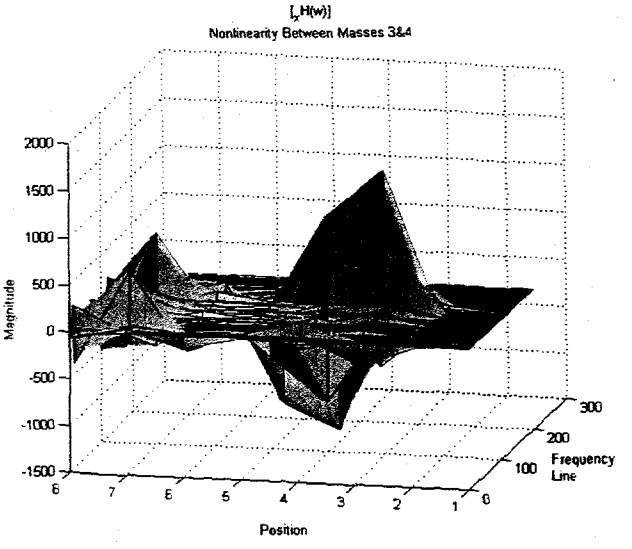

Figure 6: $[_xH(\omega)]$ Matrix Showing Nonlinearity Present Between Masses 3 & 4

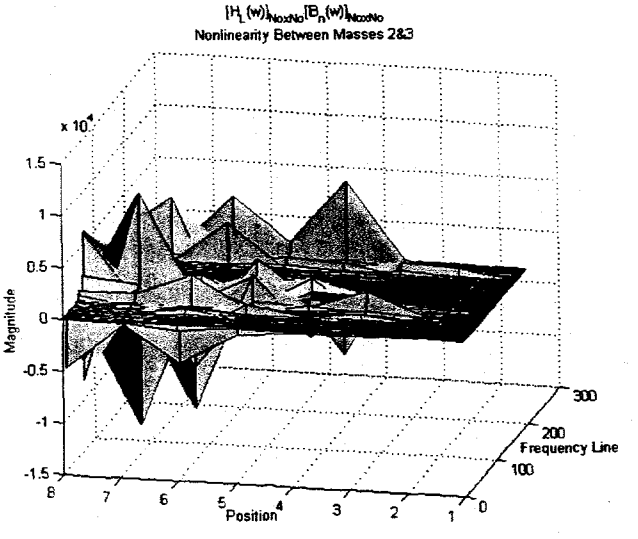

Figure 7: $[H_L(\omega)]_{NoxNo}[B_n(\omega)]_{NoxNo}$ Matrix Showing NO Peak Present Between Positions 2 & 3

2. The system was only excited with a single input instead of an input at each degree-of-freedom. Though a nonlinearity present in a system that is excited with a single input may be identified successfully, multiple inputs into the 8-dof system provide the necessary information to fully characterize a nonlinearity present at any location.
3. Adams' method relies on inverting the FRF $[H_L(\omega)]_{NoxNo}$ with only partial knowledge of $[H_L(\omega)]_{NoxNo}$. This inversion cannot be completely with a single input. The solution to this problem is to drive the system with multiple inputs. This drastically reduces the errors that are formed when the inverse is calculated in equation (9).

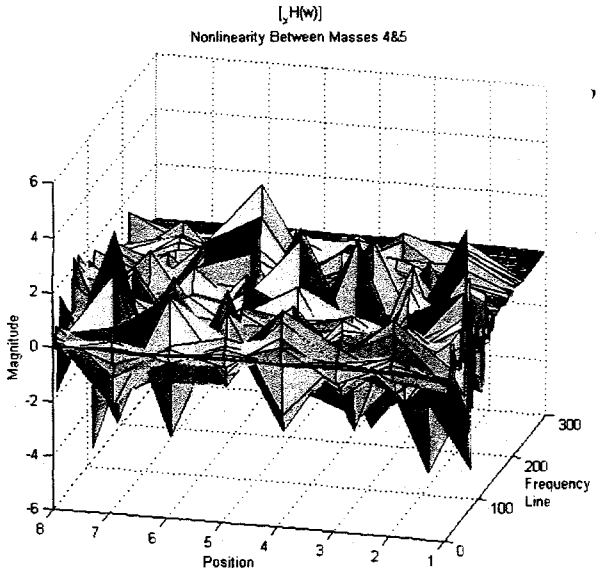

Figure 8: $[_xH(\omega)]$ Matrix Showing *NO* Nonlinearity Present Between Masses 4 & 5

Given existing time constraints, the 8-dof system could not be modified to have an input at each degree of freedom. We therefore suggest that this method be tested again after the system has been configured for multiple inputs and the friction due to the stainless steel bar be minimized or eliminated.

4. SUMMARY AND IMPORTANT ISSUES

An attempt was made to validate a method suggested by Adams in [1,5] to detect nonlinearities present in the 8-dof experimental example presented in this paper. Application of the frequency-based detection method produced inconclusive results for the mass-spring system for most scenarios presented. We conclude that this method of detection, based on a single input, is not reliable or repeatable for this experimental structural system.

Some simple changes, such as providing multiple inputs into the system instead of a single input, should theoretically produce results that show the accurate detection of nonlinearities present at any location in the structural system. This is due to the fact that the errors in the results due to numerical instability of the inverse $[H_L(\omega)]_{NoxNo}$ in equation (9) would be reduced to a minimum. In addition, if the inherent nonlinearity produced by the stainless steel bar that supports the system was reduced to a minimum, or removed altogether, the system would resemble a more linear system before the bumpers were installed. This would change all of the results obtained and would most likely detect damage at all positions.

Finally, validation on a large-scale structure is another issue that needs to be addressed before Adams' method can be truly classified as a reliable damage locator. Most damage detection methods seek to locate and repair any damage present in a structural system before failure occurs. It is perfectly acceptable to perform small laboratory experiments to determine if the method succeeds for small-scale laboratory experiments, but before being classified as a reliable structural damage detection method, validation with several different large-scale tests is required.

5. ACKNOWLEDGEMENT

The funding for this work was provided by The Department of Energy for the First Annual Los Alamos Structural Dynamics Summer School.

6. REFERENCES

[1] Adams, D. E., and Allemang, R. J., "A New Derivation of the Frequency Response Function Matrix for Vibrating Nonlinear Systems," *Journal of Sound and Vibration,* **227** (5), pp. 1083-1108, 1999.

[2] Doebling, S. W., Farrar, C. R., Prime, M. B., and Shevitz, D. W., "Damage Identification and Health Monitoring of Structural and Mechanical Systems from Changes in Their Vibration Characteristics: A Literature Review," *Los Alamos National Laboratory*, Report LA-13070-MS, 1996.

[3] Doebling, S. W., Farrar, C. R., and Prime, M. B., "A Summary Review of Vibration-Based Damage Identification Methods," *The Shock and Vibration Digest*, **30** (2), pp. 91-105, 1998.

[4] Farrar, C. R., and Doebling, S. W., "Vibration-Based Health Monitoring and Model Refinement of Civil Engineering Structures," *Proceedings of the 1st Architectural Surety Conference*, Albuquerque, NM, May 13-15, 1997.

[5] Adams, D. E., and Allemang, R. J., "A Superposition Principle for Nonlinear Systems," *Proceedings of the 18th International Modal Analysis Conference*, San Antonio, TX, February 7-10, 2000.

[6] The Math Works, Inc., *System Identification Toolbox v. 4.3 R11.1*, Natick, MA., 1999.